Microglial CSF1R radioligand [^{11}C]CPPC as a marker of disease severity in early Parkinson's disease: a pilot study.

Kelly A. Mills[1], Yong Du[2], Jennifer M. Coughlin[1,4], Andrew G. Horti[2], Katelyn Jenkins[4], Ergi Spiro[2], Chelsie S. Motley[1], Robert F. Dannals[2], Martin G. Pomper[2], Ted M. Dawson[1,5,6,7]

Affiliations:

1. Department of Neurology, Johns Hopkins University School of Medicine, Baltimore, MD 21287, USA
2. Johns Hopkins University School of Medicine, Russell H. Morgan Dept. of Radiology and Radiologic Science, Baltimore, MD, USA.
3. Johns Hopkins Center for Infection and Inflammation Imaging Research, Baltimore, MD 21287, USA.
4. Department of Psychiatry and Behavioral Sciences, Johns Hopkins University School of Medicine, Baltimore, MD 21287, USA.
5. Neuroregeneration and Stem Cell Programs, Institute for Cell Engineering, Johns Hopkins University School of Medicine, Baltimore, MD 21205, USA
6. Department of Pharmacology and Molecular Sciences, Johns Hopkins University School of Medicine, Baltimore, MD 21287, USA
7. Solomon H. Snyder Department of Neuroscience, Johns Hopkins University School of Medicine, Baltimore, MD 21205, USA

Corresponding Author:
Kelly A. Mills, M.D., M.H.S.
600 N. Wolfe Street
Meyer 6-181D
Baltimore, MD, 21287
kmills16@jhmi.edu

Funding: This work was supported by the Michael J. Fox Foundation *Grant MJFF-010064, the National Institutes of Health /* National Institute of Biomedical Imaging and Bioengineering (EB024495), and the RMS Family Foundation.

Abstract:

Background: Enhanced innate immune response is detected in autopsy studies of Parkinson's disease (PD) but the role of microglia in early pathophysiology is unclear. While the translocator protein 18 kDa (TSPO) that marks glial activation may be high in PD, TSPO expression is not limited to microglia, and ligand binding affinity for newer generation radiotracers for imaging TSPO with PET varies across individuals due to a common single nucleotide polymorphism in *TSPO*. Imaging the colony stimulating factor 1 receptor (CSF1R) with [^{11}C]CPPC PET offers an opportunity to image a complementary *in vivo* marker of microglial number and/or activity in early PD.

Objective: To determine whether the binding of [^{11}C]CPPC differs across the brains of healthy controls and patients with early PD, and to test for correlation between binding and disease severity in early PD.

Methods: Healthy controls and persons with PD of ≤2 years disease duration and Hoehn & Yahr <2.5 were enrolled. Each participant underwent motor and cognitive ratings, and then completed [^{11}C]CPPC dynamic PET with serial arterial blood sampling. The total volume of tissue distribution (V_T) in PD-relevant regions of interest was compared between groups (healthy controls, mild versus moderate PD) based on disability from motor symptoms (MDS-UPDRS Part II) and also was regressed with MDS-UPDRS Part II as a continuous measure. Correlations between V_T and cognitive measures were explored.

Results: PET imaging showed higher [^{11}C]CPPC binding in multiple regions in patients with more motor disability than those with less motor disability and compared to healthy controls. In patients with mild cognitive impairment (PD-MCI), higher CSF1R binding by [^{11}C]CPPC was associated with worse cognitive function on Montreal Cognitive Assessment (MoCA). This

inverse correlation was also found between [^{11}C]CPPC V_T and verbal fluency across the entire PD cohort.

Conclusions: Even at early stages of disease, [^{11}C]CPPC that binds the CSF1R, a direct marker of microglial density and activation, correlates with motor disability in PD and cognitive function.

Introduction:

The involvement of the innate immune system, including microglial activation of neurotoxic astrocytes[1], is increasingly recognized as playing a pathogenic role in the cascade of events associated with α-synuclein (α-Syn) misfolding and neurodegeneration in Parkinson's disease (PD). Signaling pathway abnormalities underlying microglial activation to disease-associated microglia converge with those found in genetic forms of PD[2] and neurodegenerative disease more broadly [3, 4].

Based on clinicopathologic analyses of autopsy tissue [5] and the model of fibrillar α-Syn injection in mice [6], the spreading proteinopathy hypothesis holds that fibrillar α-Syn seeds and templates wild type protein, causing toxic intracellular aggregation. Propagation of α-Syn fibrillation and cell to cell spread of pathologic α-Syn is driven, in part, by the innate immune response [7]. Once oligomerized, fibrillar α-Syn activates microglia [8, 9], creating a cycle of neuroinflammation and neurodegeneration.

With the interplay between innate immunity and pathogenic α-Syn in the spread of pathologic α-Syn throughout the brain, suppressing this immune activation may be critical for disease modification in PD [7]. A key step in developing targeted therapies to this end is development of an *in vivo* measure of microglial activity and proliferation that is specific to the cell type and processes of interest. To date, human *in vivo* assessment of CNS immune activation has involved nuclear medicine radiotracers targeting the translocator protein 18 kDa (TSPO)[10], but limitations of these radiotracers and the TSPO target complicate the inference of direct microglial density and activation. First generation TSPO ligands like [^{11}C](*R*)-PK11195 have a poor signal to noise ratio and highly variable kinetic behavior[11]. Newer TSPO

radiotracers like [^{11}C]DPA-713 have much better signal-to-noise but are susceptible to low affinity in persons with a specific TSPO single nucleotide polymorphism[12]. More recently, it has also been shown that TSPO expression is not limited to microglia. For example, TSPO expression increases in astrocytes before microglia[13], may be present in neurons[14], and may increase with neuronal activation[15].

As a microglia-specific alternative to TSPO imaging, our team developed a radiotracer[16] that targets the colony stimulating factor 1 receptor (CSF1R), a tyrosine kinase involved in proliferation and activation of microglia. The CSF1R is largely only expressed by microglia and infiltrating macrophages in the CNS. This radiotracer, [^{11}C]CPPC, has been shown to have faster kinetics and less off-target cerebellar binding than another leading candidate radiotracer, [^{11}C]GW2580, which also shows tracer kinetics suboptimal for use in humans due to long scan times[17]. [^{11}C]CPPC regional volume of distribution (V_T) values can be well estimated in health human subjects[18], suggesting its use as a radiotracer in immune-mediated disease states.

Given the need for in vivo assessment of microglial density and proliferation at early stages of neurodegeneration in PD to establish causality and potentially, as a biomarker for target engagement in disease modification trials, we studied [^{11}C]CPPC in a cohort of persons with early Parkinson's disease and age-similar healthy controls. Our goal was to describe the relationship between PD disease severity and [^{11}C]CPPC binding as a cell-type specific marker of microglia.

Methods:

Subjects: We enrolled persons between ages 50-80 with a clinically established Parkinson's disease[19] within 2 years of diagnosis and with Hoehn and Yahr stage 2 or lower. People in this state of disease are fully ambulatory and mostly independent. Healthy subjects age 50-80 were recruited from PD and PD caregiver support groups, families of persons with PD, or the general public. We excluded potential participants with other systemic autoimmune disorders, recent

infection, anti-inflammatory or immunosuppressant use, a history of moderate or severe TBI, or other known neurodegenerative diseases. Safety labs, including chemistry panel, liver function tests, serum pregnancy test (if female and premenopausal), and EKG were performed and patients were excluded for lab values >1.5 times the upper limit of normal. The study was performed with approval by the Johns Hopkins Institutional Review Board and was compliant with the Declaration of Helsinki. Patients underwent informed consent prior to participation in the study protocol.

At the baseline visit, all participants underwent examination for parkinsonism and if absent, the Prodromal PD Calculator was administered and healthy controls were only enrolled as such if the likelihood ratio for prodromal PD did not meet or exceed that which would provide 80% likelihood of eventual PD, stratified by age[20, 21], and if they did not meet criteria for clinically established Parkinson's disease[19]. Participants with a prior diagnosis of PD were examined for parkinsonism and if present, the Movement Disorder Society Clinical Diagnostic Criteria for Parkinson's Disease were applied. Those meeting criteria for clinically established Parkinson's disease were enrolled in the "Parkinson's disease" cohort.

Clinical Assessments: All participants underwent the Movement Disorders Society-Unified Parkinson's Disease Rating Scale (MDS-UPDRS) parts I-IV in the medicated state. Other assessments included Montreal Cognitive Assessment (MoCA), phonemic (letter) verbal fluency, Beck Depression Rating Scale-2, University of Pennsylvania Smell Identification Test, in addition to a medical history and medication history. Participants with PD were classified as having mild cognitive impairment (PD-MCI) by level 1 criteria[22] if they had a subjective report of cognitive impairment (MDS-UPDRS part 1, question 1 ≥1) and an abnormal measure of global cognitive impairment (MoCA<26).

MRI: Participants received a brain MRI for PET co-registration and to screen for anatomic variations or lesions that would preclude analysis of PET data at a group level. MRI's were

performed on a Philips dStream Ingenia Elition 3T with a 3D-acquired T1-wieghted sequence, T2 sequence, and iron-sensitive sequences. FreeSurfer[23] image analysis suite was used for automated segmentation of MRI into regions of interest (ROIs) in PD: brainstem, total grey matter, cerebellum, thalamus, striatum, hippocampus, corpus callosum, temporal cortex, occipital cortex, cingulate, frontal cortex, parietal cortex, caudate, putamen, pallidum, anterior cingulate cortex, and posterior cingulate cortex.

PET Imaging: The synthesis of [^{11}C]CPPC occurred in the Johns Hopkins PET Center, where radiochemical purity was confirmed at >95%[16]. The target injection radioactivity was 740 MBq, with a max of 777 MBq and minimum of 703 MBq. Participants were fitted with a thermoplastic face mask to minimize head motion. A radial arterial catheter was inserted for serial arterial blood sampling and an intravenous catheter was inserted for PET radiotracer injection. A 128-slice low-dose CT was administered for attenuation correction before the injection. A 90-minute emission scan on a Siemens Biograph mCT PET/CT began with IV injection of 740 MBq of [^{11}C]CPPC. Serial arterial blood was at first drawn as fast as possible for 90 seconds, then at increasingly longer intervals between blood samples thereafter. Select samples at (5, 10, 20, 30, 60, and 90 minutes were analyzed with high performance liquid chromatography (HPLC) for radioactive plasma metabolites [18]. Thirty frames (four of 15 seconds, four of 30 seconds, three of 1 minute, two of 2 minutes, 5 of 4 minutes, and twelve of 5 minutes) from the 90 minutes emission scan were reconstructed using the iterative ordered subset expectations maximization algorithm and corrected for attenuation, randoms, scatter, and time-of-flight. PET data processing and tracer kinetic modeling were performed as previously described[18] using PMOD (v3.7, PMOD Technologies Ltd., Zurich, Switzerland). Briefly, inter-frame motion correction was first applied by frame-by-frame matching to a reference frame generated from the average of the frames from 30-60 minutes post-injection. Next, the PET data were transformed to MRI space through rigid registration. The MRI segmented ROIs were then applied to the registered PET images to generate a time activity curve for each region. The total distribution volume V_T,

which reflects the equilibrium ratio of [^{11}C]CPPC concentration in tissue to the concentration in arterial plasma was finally calculated using Logan graphical analysis[24] with metabolite corrected plasma input function.

Statistical analyses: For human PET imaging, summary statistics were used to describe mean clinical variable values or proportions in the healthy control and PD groups. Independent samples t-tests were used to evaluate the difference in V_T between healthy controls and participants with PD in each ROI. Given a high degree of heterogeneity in regional V_T in the PD group, multiple linear regression was performed for each region of interest, regressing [^{11}C]CPPC V_T on disease severity measured by the MDS-UPDRS Part II, the most clinically relevant measure of disease severity [25], adjusting for age at the time of PET scan. Based on findings from this analysis, PD participants were stratified in the motor severity domain into "mild" disease (≤ median MDS-UPDRS Part II score of 4) or "moderate" disease (>median MDS-UPDRS Part II score of 4). ANCOVA was performed for each region of interest to test for any difference in variance of V_T between 3 groups: healthy controls, "mild" PD, or "moderate" PD. To further explore the heterogeneity of [^{11}C]CPPC V_T in PD participants as it relates to variance in the cognitive domain, regional V_T was regressed onto a global measure of cognition (MoCA) in participants with and without MCI.

Given that this is a first-in-PD pilot study using [11C]CPPC PET to image the CSF1R, the statistical significance of results was not adjusted to account for the multiple regions tested.

Results:

We consented 10 controls but excluded one due to recent COVID19 infection within the past two weeks and excluded another because of cognitive complaints within domains of memory and executive function. We consented and enrolled nine participants with PD, all with a Hoehn and Yahr score of 2 or lower and within two years of diagnosis. Of the nine PD participants, four

had PD-MCI based on our criteria. In addition, of the nine PD participants, five had “mild” and four had “moderate” disability from motor symptoms based on whether they were below or above the median MDS-UPDRS-II score, respectively. Clinical characteristics of these groups are in Table 1.

The mean [^{11}C]CPPC V_T was computed using the Logan method and plotted across ROIs in healthy controls and those with both mild- or moderate-PD based on disability from motor symptoms quantified by the MDS-UPDRS part II (Figure 2). ANCOVA testing for the difference in mean V_T between these groups, adjusting for age, showed significant difference by group in the cerebellar cortex (F=3.98, p=0.43), striatum (F=5.03, p=0.023), caudate nucleus (F=4.23, p=0.037), and putamen (F=5.19, p=0.021) and there was a trend for a difference across groups in the temporal cortex (F=3.4, p=0.063). Tukey’s post hoc testing showed that this difference was driven by the difference between the moderate motor disability and mild motor disability groups and between moderate motor disability and control groups ($p<0.05$ for all pair-wise tests). No regions showed a statistically significant difference between healthy controls and mild motor disability groups in a group-wise comparison but V_T in multiple regions showed a positive association with motor-related disability when used as a continuous variable in multiple linear regressions adjusted for age. Greater motor disability was associated with higher [^{11}C]CPPC binding in the brainstem, cerebellar cortex, hippocampus, temporal cortex, cingulate cortex, caudate nucleus, and posterior cingulate cortex (Table 2). While the models for total grey matter, thalamus, occipital cortex, frontal cortex, and parietal cortex did not meet statistical significance, the individual β-coefficients for V_T was <0.05 in these models as well. Representative scatter plots fit with a linear representation of the association, adjusted for age, are seen in Figure 3.

Participants with PD were also stratified by cognitive status, and at a group level, [^{11}C]CPPC was not higher in any region in participants with PD-MCI than those with PD-NC or

healthy controls (ANOVA $p>0.05$ for all regions). [^{11}C]CPPC V_T was also regressed on performance on a global measure of cognitive function, MoCA, adjusting for age. Using the entire cohort of patients with PD (N=9), there was no association between MoCA and V_T in any of the regions tested. Because this cohort has early PD, there was a ceiling effect of the MoCA with 4 of 5 PD-NC patients having a 28 or 29 out of 30 total possible points. Restricting the analysis to those with PD-MCI (N=4) to avoid a ceiling effect of cognitive performance, multiple regions showed inverse correlation between MoCA and V_T (Table 3) but only the caudate showed a statistically significant association between MoCA and V_T when adjusting for age ($F_{model} = 247$, $\beta_{caudate} = -6.97$, $p = 0.035$). In the entire PD cohort, regardless of cognitive status, worse verbal fluency was associated with higher [^{11}C]CPPC V_T in multiple linear regression adjusted for age (Table 4).

Discussion:

In response to the substantial heterogeneity in clinical presentation and pathogenic mechanisms in PD, precision medicine strategies are being sought to identify clinical subtypes of PD and target that subtype with relevant disease-modifying strategy. Especially in sporadic PD, an increasing focus has been placed on the role of innate CNS immunity, potentially interacting with peripheral T cell response and adaptive immunity. This pilot study presents early data on the use of [^{11}C]CPPC, which targets the CSF1R expressed on microglia and peripheral macrophages in the CNS. High CSF1R is associated with LPS-induced neuroinflammation, and may prove a useful imaging marker of microgliosis. This study adds to the growing literature on timing of microglial response by showing correlations between microglial proliferation and motor and cognitive disease severity in PD even at an early stage.

These data build on previous work that showed elevation of TSPO in PD participants versus those without known neurodegeneration using PET, but several issues complicate the use of these ligands in research and as potential biomarkers of innate immunity: Though most

highly expressed in activated microglia, TSPO may be increased in expression by activated astrocytes even before increased TSPO expression by microglia in neurodegeneration.[13] TSPO may also be found in neurons where it increases with neuronal activation[15]. While initial studies with [^{11}C]-PK11195 showed higher binding in PD versus controls[26], a subsequent study showed overlap between PD and healthy controls and that treatment with an anti-inflammatory unexpectedly *increased* binding potential in the same brain regions[27]. While not susceptible to genetic variation in TSPO binding affinity like later generation TSPO ligands, [^{11}C]-PK11195 also has a low signal-to-noise ratio due to off-target binding[28]. Later generation TSPO ligands like [^{18}F]DPA-714 have higher affinity but this affinity can be substantially reduced by a SNP in the TSPO gene. In a large study looking comparing [^{18}F]DPA-714 binding in people with PD and controls, even after persons with low affinity were excluded based on genotyping, significant differences in binding between PD and controls were only found in the 40 high-affinity binders, but not in the 27 mixed-affinity binders[29]. This would mean that use of new generation TSPO ligands to diagnose those elevated innate immunity or to track microglial activation after an intervention would be limited to high-affinity binders, which are expected to comprise only 49% of the population[12]. In our older, healthy controls, and in the least-affected PD group, the variance in binding was relatively small without outliers to suggest high natural variance in binding. Thus, our finding of a potentially more specific marker of microglial activation that is not known to have genetic variation in binding affinity for its target, represents a more specific, reliable marker of the microglial proliferation and/or activation in PD.

While this correlative study cannot establish a causal link between microglial activation and α-synuclein-related neurodegeneration, it aligns with preclinical and neuropathological evidence that supports a contributory role in cell death. Microgliosis precedes cell death in α-synuclein over-expression animal models [30] and in human autopsy studies[31] and at least two mechanisms have been proposed: 1) direct or indirect (via activated astrocytes) toxicity to

neurons via α-synuclein-activated microglia [1, 31, 32] and 2) microglia-mediated enhancement of α-synuclein oligomerization[33] and spread throughout the brain[34, 35]. Since some of the most promising disease-modifying agents in PD[36] are thought to act via microglia[7], having an *in vivo* biomarker for microglial activity may facilitate therapy development and hasten drug trials as an indicator of target engagement in proof-of-principle studies and clinical trials.

While this study shows promising signal with the first use of a CSF1R ligand in PD versus controls, there are limitations to consider in the interpretation of these data. The sample size is small and we are at risk for a type II statistical error in looking for group-wise differences in [^{11}C]CPPC binding between PD and control participants. On the other hand, the strength of linear correlations with measures of disease severity is encouraging. The study's cross-sectional nature limits our ability to truly understand the relationship between [^{11}C]CPPC binding and disease severity within individuals, but the cross-sectional pilot data warrant future research in this regard. Our analysis included statistical testing between groups across 15 regions of interest, increasing the false discover rate. However, this exploratory analysis is important to disseminate in order to potentially guide the design of future studies with this or other radiotracers targeting CSF1R so that target regions of interest can be identified for future studies.

In conclusion, these data suggest that using [^{11}C]CPPC as a radioligand of CSF1R can detect microgliosis in early PD with at least moderate severity in a small cohort of patients, and that variance in [^{11}C]CPPC binding within patients with PD correlates with disability from motor dysfunction and possible, cognitive impairment in those with MCI. As a potential alternative to TSPO PET ligands, [^{11}C]CPPC could be useful for identifying potential participants with microgliosis for trials that target immune activation in PD or for evaluating target engagements in such studies.

Acknowledgement: The authors would like to thank the PET Radiotracer Center staff (Andrew Hall, Hong Fan, Daniel P. Holt, and William B. Mathews) for their expertise in the synthesis of the radiotracer used in this study and the PET Center staff (Karen Edmonds) for her scanning expertise.

Disclosures:

Drs. Kelly Mills, Yong Du, and Robert Dannals as well as Katelyn Jenkins, Chelsie Motley, and Ergi Sprio report no competing interest. Under a license agreement between D&D Pharmatech and the Johns Hopkins University, the University and Drs. Pomper, Coughlin and Horti are entitled to royalty distributions related to the technology described in the study discussed in this publication. Drs. Pomper and Horti are founders of and hold equity in D&D Pharmatech. He and Dr. Horti are also paid consultants to the company. This arrangement has been reviewed and approved by the Johns Hopkins University in accordance with its conflict of interest policies. Dr. Dawson holds shares of stock options as well as equity in D & D Pharmatech; These arrangements have been reviewed and approved by the Johns Hopkins University in accordance with its conflict of interest policies.

References:

1. Liddelow SA, Guttenplan KA, Clarke LE, et al. Neurotoxic reactive astrocytes are induced by activated microglia. Nature 2017;541:481-487. PMC5404890
2. Mamais A, Kaganovich A, Harvey K. Convergence of signalling pathways in innate immune responses and genetic forms of Parkinson's disease. Neurobiol Dis 2022;169:105721.

3. Krasemann S, Madore C, Cialic R, et al. The TREM2-APOE Pathway Drives the Transcriptional Phenotype of Dysfunctional Microglia in Neurodegenerative Diseases. Immunity 2017;47:566-581.e569. PMC5719893
4. Panicker N, Kam TI, Wang H, et al. Neuronal NLRP3 is a parkin substrate that drives neurodegeneration in Parkinson's disease. Neuron 2022;110:2422-2437.e2429. PMC9357148
5. Braak H, Del Tredici K, Rub U, de Vos RA, Jansen Steur EN, Braak E. Staging of brain pathology related to sporadic Parkinson's disease. Neurobiol Aging 2003;24:197-211.
6. Luk KC, Kehm V, Carroll J, et al. Pathological alpha-synuclein transmission initiates Parkinson-like neurodegeneration in nontransgenic mice. Science 2012;338:949-953. 3552321
7. Yun SP, Kam TI, Panicker N, et al. Block of A1 astrocyte conversion by microglia is neuroprotective in models of Parkinson's disease. Nat Med 2018;24:931-938. PMC6039259
8. Kim C, Ho DH, Suk JE, et al. Neuron-released oligomeric α-synuclein is an endogenous agonist of TLR2 for paracrine activation of microglia. Nature communications 2013;4:1562. PMC4089961
9. Duffy MF, Collier TJ, Patterson JR, et al. Lewy body-like alpha-synuclein inclusions trigger reactive microgliosis prior to nigral degeneration. Journal of neuroinflammation 2018;15:129. PMC5930695
10. Werry EL, Bright FM, Piguet O, et al. Recent Developments in TSPO PET Imaging as A Biomarker of Neuroinflammation in Neurodegenerative Disorders. International journal of molecular sciences 2019;20. PMC6650818
11. Chen MK, Guilarte TR. Translocator protein 18 kDa (TSPO): molecular sensor of brain injury and repair. Pharmacol Ther 2008;118:1-17. PMC2453598
12. Owen DR, Yeo AJ, Gunn RN, et al. An 18-kDa translocator protein (TSPO) polymorphism explains differences in binding affinity of the PET radioligand PBR28. J Cereb Blood Flow Metab 2012;32:1-5. PMC3323305
13. Tournier BB, Tsartsalis S, Ceyzériat K, et al. Astrocytic TSPO Upregulation Appears Before Microglial TSPO in Alzheimer's Disease. J Alzheimers Dis 2020;77:1043-1056. PMC7683091
14. Gong J, Szego É M, Leonov A, et al. Translocator Protein Ligand Protects against Neurodegeneration in the MPTP Mouse Model of Parkinsonism. J Neurosci 2019;39:3752-3769. PMC6510339
15. Notter T, Schalbetter SM, Clifton NE, et al. Neuronal activity increases translocator protein (TSPO) levels. Mol Psychiatry 2021;26:2025-2037. PMC8440208 Ingelheim Pharma GmbH & Co. and from and Wren Therapeutics Ltd; and JH has had financial support from Pfizer Inc., Wyeth, Astra-Zeneca, Abbvie and Takeda Pharmaceutical. All authors declare no conflicts of interests.
16. Horti AG, Naik R, Foss CA, et al. PET imaging of microglia by targeting macrophage colony-stimulating factor 1 receptor (CSF1R). Proc Natl Acad Sci U S A 2019;116:1686-1691. PMC6358677
17. Zhou X, Ji B, Seki C, et al. PET imaging of colony-stimulating factor 1 receptor: A head-to-head comparison of a novel radioligand, (11)C-GW2580, and (11)C-CPPC, in mouse models of acute and chronic neuroinflammation and a rhesus monkey. J Cereb Blood Flow Metab 2021;41:2410-2422. PMC8393303
18. Coughlin JM, Du Y, Lesniak WG, et al. First-in-human use of (11)C-CPPC with positron emission tomography for imaging the macrophage colony-stimulating factor 1 receptor. EJNMMI research 2022;12:64. PMC9522955
19. Postuma RB, Berg D, Stern M, et al. MDS clinical diagnostic criteria for Parkinson's disease. Mov Disord 2015;30:1591-1601.
20. Berg D, Postuma RB, Adler CH, et al. MDS research criteria for prodromal Parkinson's disease. Mov Disord 2015;30:1600-1611.
21. Heinzel S, Berg D, Gasser T, Chen H, Yao C, Postuma RB. Update of the MDS research criteria for prodromal Parkinson's disease. Mov Disord 2019;34:1464-1470.

22. Litvan I, Goldman JG, Troster AI, et al. Diagnostic criteria for mild cognitive impairment in Parkinson's disease: Movement Disorder Society Task Force guidelines. Mov Disord 2012;27:349-356. 3641655
23. Fischl B, Salat DH, Busa E, et al. Whole brain segmentation: automated labeling of neuroanatomical structures in the human brain. Neuron 2002;33:341-355.
24. Logan J, Fowler JS, Volkow ND, et al. Graphical analysis of reversible radioligand binding from time-activity measurements applied to [N-11C-methyl]-(-)-cocaine PET studies in human subjects. J Cereb Blood Flow Metab 1990;10:740-747.
25. Bouça-Machado R, Fernandes A, Ranzato C, Beneby D, Nzwalo H, Ferreira JJ. Measurement tools to assess activities of daily living in patients with Parkinson's disease: A systematic review. Front Neurosci 2022;16:945398. PMC9386643
26. Edison P, Ahmed I, Fan Z, et al. Microglia, amyloid, and glucose metabolism in Parkinson's disease with and without dementia. Neuropsychopharmacology 2013;38:938-949. PMC3629382
27. Bartels AL, Willemsen AT, Doorduin J, de Vries EF, Dierckx RA, Leenders KL. [11C]-PK11195 PET: quantification of neuroinflammation and a monitor of anti-inflammatory treatment in Parkinson's disease? Parkinsonism Relat Disord 2010;16:57-59.
28. Petit-Taboué MC, Baron JC, Barré L, et al. Brain kinetics and specific binding of [11C]PK 11195 to omega 3 sites in baboons: positron emission tomography study. Eur J Pharmacol 1991;200:347-351.
29. Yacoubian TA, Fang YD, Gerstenecker A, et al. Brain and Systemic Inflammation in De Novo Parkinson's Disease. Mov Disord 2023.
30. Watson MB, Richter F, Lee SK, et al. Regionally-specific microglial activation in young mice over-expressing human wildtype alpha-synuclein. Exp Neurol 2012;237:318-334. PMC3443323
31. Sanchez-Guajardo V, Barnum CJ, Tansey MG, Romero-Ramos M. Neuroimmunological processes in Parkinson's disease and their relation to α-synuclein: microglia as the referee between neuronal processes and peripheral immunity. ASN Neuro 2013;5:113-139. PMC3639751
32. Jiang T, Xu C, Gao S, et al. Cathepsin L-containing exosomes from α-synuclein-activated microglia induce neurotoxicity through the P2X7 receptor. NPJ Parkinson's disease 2022;8:127. PMC9537534
33. Gao HM, Kotzbauer PT, Uryu K, Leight S, Trojanowski JQ, Lee VM. Neuroinflammation and oxidation/nitration of alpha-synuclein linked to dopaminergic neurodegeneration. J Neurosci 2008;28:7687-7698. PMC2702093
34. Guo M, Wang J, Zhao Y, et al. Microglial exosomes facilitate α-synuclein transmission in Parkinson's disease. Brain 2020;143:1476-1497. PMC7241957
35. George S, Rey NL, Tyson T, et al. Microglia affect α-synuclein cell-to-cell transfer in a mouse model of Parkinson's disease. Molecular neurodegeneration 2019;14:34. PMC6697982
36. Athauda D, Maclagan K, Skene SS, et al. Exenatide once weekly versus placebo in Parkinson's disease: a randomised, double-blind, placebo-controlled trial. Lancet 2017;390:1664-1675. PMC5831666

	Controls		PD-all		PD-NC		PD-MCI		PD-Mild		PD-Moderate	
N	8		9		5		4		5		4	
	μ	SD	μ	SD	μ	SD	μ	SD	μ	SD	μ	SD
Age (yr)	65.6	4.6	67.9	5.6	68.2	6.9	67.6	4.4	66.1	7.1	70.2	1.7
Levodopa (mg/day)	0.0	0.0	336	185	440	151	206	142	305	62	375	287
MDS-UPDRS III	3.4	2.3	22.9	4.9	21.4	5.5	24.8	3.9	22.2	2.9	23.8	7.1
MDS-UPDRS II	0.1	0.4	5.2	4.5	6.2	4.8	4.0	4.3	2.0	1.6	9.3	3.3
MoCA	26.8	3.1	26.1	2.5	28.0	1.2	23.8	1.3	25.4	1.7	27.0	3.4
BDI-2	2.4	2.6	7.2	4.6	7.0	4.2	7.5	5.7	5.8	4.9	9.0	4.1

Table 1. Demographics in groups stratified by disease status (PD-all = all participants with clinically established Parkinson's disease (PD)) or disease severity. PD-NC = PD with normal cognition; PD-MCI = PD with mild cognitive impairment by level 1 criteria; PD-Mild = PD with ≤ median score for cohort on MDS-UPDRS Part II; PD-Moderate = PD with > median score for cohort on MDS-UPDRS Part II.

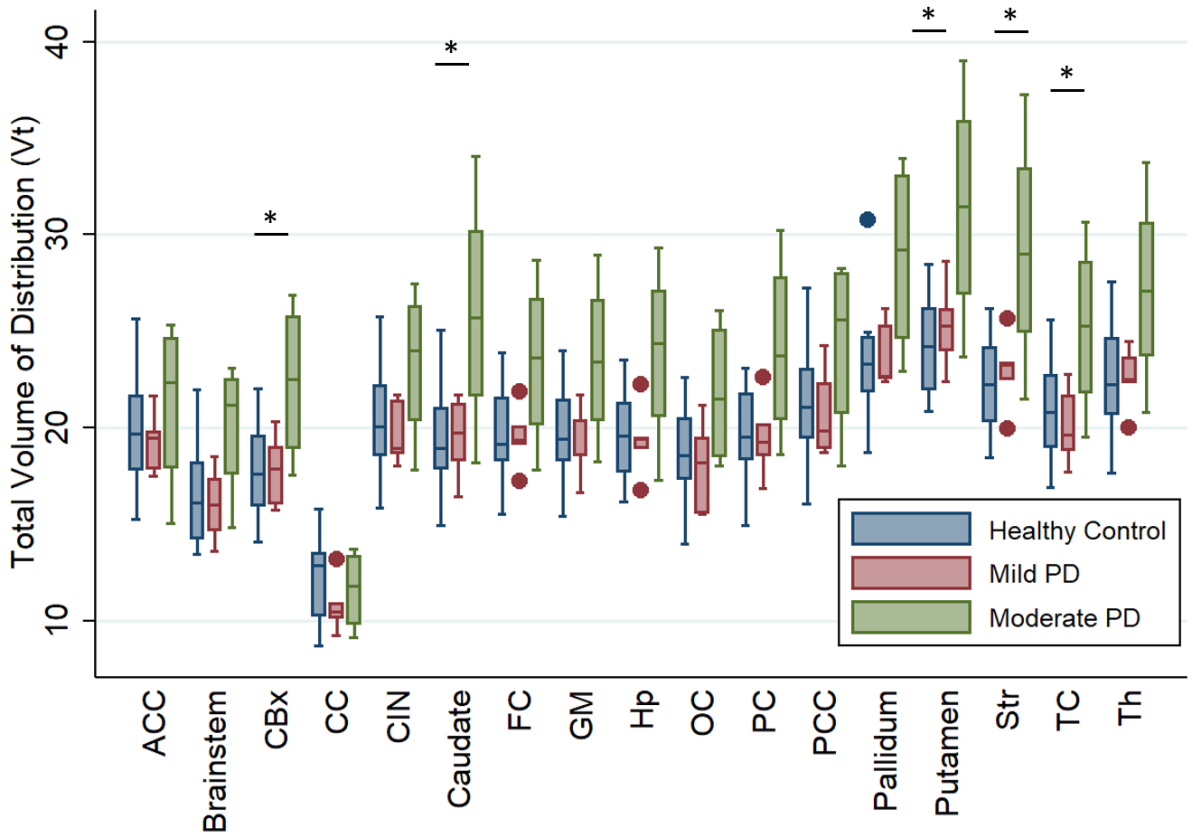

Figure 2. Freesurfer-based regional total volume of distribution (V_T) of [^{11}C]CPPC, a CSF1R PET radioligand, in people with mild or moderate PD, defined by disability from motor symptom severity, and controls of a similar age. * = p<0.05 for ANOVA and post-hoc test between Moderate PD vs. Mild PD and Moderate PD vs. Healthy Controls. ACC = anterior cingulate cortex, CBx = cerebellar cortex, CC = corpus callosum, CIN = cingulate cortex, FC = frontal cortex, GM = grey matter, Hp = hippocampus, OC = occipital cortex, PC = parietal cortex, PCC = posterior cingulate cortex, Str = striatum, TC = temporal cortex, Th = thalamus

Region	β	p
Brainstem	0.640	0.008
Cerebellar cortex	0.716	0.010
Hippocampus	0.642	0.032
Temporal cortex	0.771	0.013
Cingulate cortex	0.631	0.014
Caudate	0.786	0.046
Posterior cingulate cortex	0.715	0.015

Table 2. Results of multiple linear regression of MDS-UPDRS Part 2 on regional [^{11}C]CPPC VT in 9 persons with Parkinson's disease, adjusted for age.

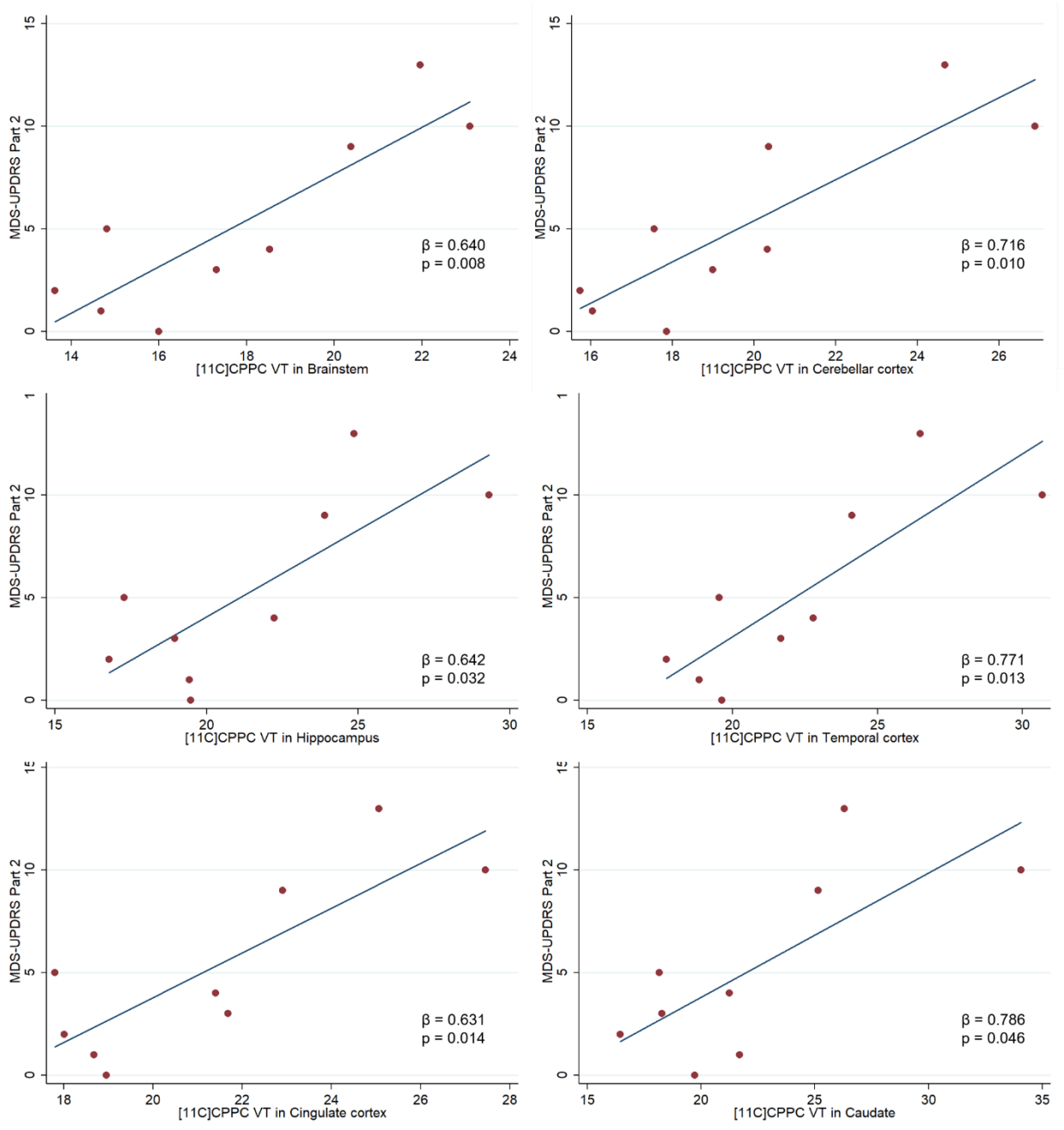

Figure 3. Scatter plots and linear relationship between [^{11}C]CPPB V_T and ADL disability from motor symptoms, measured by MDS-UPDRS Part 2 in regions of interest that showed a statistically significant relationship, adjusting for age.

Region	r	p
Brainstem	-0.96	0.04*
Grey matter	-0.97	0.03*
Cerebellar Cortex	-0.98	0.02*
Thalamus	-0.99	0.01*
Striatum	-0.99	0.01*
Hippocampus	-0.98	0.02*
Corpus callosum	-0.82	0.18
Temporal cortex	-0.97	0.03*
Occipital cortex	-0.96	0.04*
Cingulate	-0.96	0.04*
Frontal cortex	-0.97	0.03*
Parietal cortex	-0.97	0.03*
Caudate	-0.99	0.01*†
Putamen	-0.99	0.01*
Pallidum	-0.99	0.01*
Anterior cingulate	-0.96	0.04*
Posterior cingulate	-0.91	0.09

Table 3. Correlation between regional [^{11}C]CPPC V_T and MoCA in 4 persons with PD-MCI. *p<0.05 for Pearson correlation. †p<0.05 for multiple linear regression adjusting for age.

Region	β	p	
Brainstem	-0.20	0.04	*
Grey matter	-0.20	0.08	
Cerebellar Cortex	-0.22	0.04	*
Thalamus	-0.21	0.09	
Striatum	-0.26	0.08	
Hippocampus	-0.21	0.07	
Corpus callosum	-0.06	0.33	
Temporal cortex	-0.23	0.06	
Occipital cortex	-0.22	0.03	*
Cingulate	-0.18	0.08	
Frontal cortex	-0.18	0.09	
Parietal cortex	-0.22	0.06	
Caudate	-0.22	0.15	
Putamen	-0.30	0.04	*
Pallidum	-0.24	0.04	*
Anterior cingulate	-0.11	0.33	
Posterior cingulate	-0.21	0.07	

Table 4. Results of multiple linear regression of verbal fluency on regional [^{11}C]CPPC V_T 9 persons with PD, adjusted for age. *p<0.05